Data-based evaluation of direction reconstruction for IceCube cascade events by utilizing starting tracks

Downloaded from: https://research.chalmers.se, 2025-06-09 14:31 UTC

Citation for the original published paper (version of record):

Abbasi, R., Ackermann, M., Adams, J. et al (2024). Data-based evaluation of direction reconstruction for IceCube cascade events by utilizing
starting tracks. Proceedings of Science, 444

N.B. When citing this work, cite the original published paper.

research.chalmers.se offers the possibility of retrieving research publications produced at Chalmers University of Technology. It covers all kind of research output: articles, dissertations, conference papers, reports etc. since 2004. research.chalmers.se is administrated and maintained by Chalmers Library

(article starts on next page)

PROCEEDINGS OF SCIENCE

Data-based evaluation of direction reconstruction for IceCube cascade events by utilizing starting tracks

The IceCube Collaboration

(a complete list of authors can be found at the end of the proceedings)

E-mail: yosuke.ashida@icecube.wisc.edu

The IceCube Neutrino Observatory instruments a cubic-kilometer of glacial ice and has been the first experiment to identify high-energy astrophysical neutrinos. There are two main morphologies of IceCube events: tracks and cascades. Tracks result from muons, while cascades result from particle showers induced by in-ice interactions. The directional reconstruction of cascades is less precise than that of tracks, which limits the sensitivity of astrophysical neutrino analyses with cascade events. In order to improve the directional reconstruction of cascade events, accurate ice modeling is essential. However, potential biases might exist in data stemming from unconstrained systematic uncertainties. In this work, feasibility studies to better understand the ice using a data-driven approach are performed, where photons that are likely to have been induced by the hadronic cascade part of muon neutrino charged-current interactions are categorized using probability density functions in time, distance and angle, and the reconstructed direction with this *pseudo-cascade* is compared with the track direction. In this proceedings, methodology and results are detailed and a path towards better understanding of the ice is discussed.

Corresponding authors: Yosuke Ashida[1*]

[1] *Department of Physics and Astronomy, University of Utah*

[*] Presenter

The 38th International Cosmic Ray Conference (ICRC2023)
26 July – 3 August, 2023
Nagoya, Japan

© Copyright owned by the author(s) under the terms of the Creative Commons Attribution-NonCommercial-NoDerivatives 4.0 International License (CC BY-NC-ND 4.0).

PoS(ICRC2023)980

1. Introduction

The IceCube Neutrino Observatory provides important science results, e.g., the discovery of astrophysical neutrinos [1]. It instruments a cubic-kilometer of glacial ice at the geographic South Pole and consists of 5,160 digital optical modules (DOMs) in 86 vertical drill holes to detect Cherenkov light emitted from relativistic charged particles traveling inside ice. Observed neutrino events in IceCube can be categorized into two main morphologies: tracks from high-energy muons produced in ν_μ charged-current (CC) interactions and cascades from neutral-current (NC) interactions or ν_e/ν_τ CC interactions. Due to their large extension, track directions are inferred much more precisely than cascades. In IceCube, the directional pointing accuracy is usually deduced from Monte-Carlo (MC) simulation as no reference point sources are available. Cosmic ray absorption by the Moon leads to a localized deficit of muons in the sky, but this is only useful for track events and is also limited by the fact that the Moon is not a point source [2].

In this work, a data-based method is employed by comparing cascade directions to tracks on a per-event basis in order to probe ice model effects (see Ref. [3] for the preceding work that motivated the present study). Here, a selection comprised of predominantly ν_μ CC interactions is utilized. Such events are deep inelastic and composed of an initial hadronic cascade in addition to an outgoing muon track. On average, the track and cascade directions are expected to be aligned at high energies ($E_\nu \gtrsim 1$ TeV). For each event, the detected photons are split into those likely to have been produced by the hadronic cascade and those likely emitted by the outgoing muon. The hadronic part of the event is reconstructed with a cascade reconstruction algorithm and the resulting direction is compared to the reconstructed track direction. A newly developed sample based on the starting track selection (ESTES) [4–7], specifically the one tailored for the neutrino source analysis, is used. The benefit of using this sample is that a high purity of ν_μ CC events is achieved (~97% for the entire sample) with most events having sufficient track length for accurate reconstruction. The performance of track reconstruction in this sample is high; the median standard deviation evaluated by MC is as good as 0.5 degrees in both zenith and azimuth directions, hence the track direction can be used well as a reference for the cascade direction. Based on MC, the median neutrino energy of the sample is around 2 TeV, thus the median hadronic shower energy on which this result is based will be a fraction of that.

2. Photon Selection and Cascade Reconstruction

Cherenkov photons contributing to each detected event are categorized into those likely to have originated from the initial hadronic cascade and otherwise. This is achieved based on log-likelihood ratios (rlogL) calculated using probability density functions (PDFs). Two types of 2D PDFs are prepared: arrival time vs. distance, and opening angle vs. distance. Figure 1 shows photon arrival times as a function of distance from the reconstructed interaction vertex, for simulated ν_μ CC starting events at ESTES final level, with the photon propagation being based on the ice model Spice 3.2.1. The emission of Cherenkov photons from the initial hadronic cascade only happens close to the interaction vertex (up to ~10 m) while the muon emits light continuously along its trajectory. The distributions look as expected and are normalized so as to be used as PDFs later. Secondly, as shown in Figure 2, the opening angle between the reconstructed muon direction and

PoS(ICRC2023)980

the vector from the vertex to a detecting DOM is taken as a parameter and plotted for different distances from the interaction vertex. It is found that the hadronic cascade-originated photons are detected around the vertex and in a wide angle range because the initial hadron and its daughter particles undergo multiple scattering. In contrast, the muon-originated photons are mainly detected far away from the vertex, which distribute at small opening angles in the figure. The rlogL is then calculated for each detected photon using these PDFs as,

$$\mathrm{rlogL} = \log\left(\frac{L_h}{L_\mu}\right),\ L_h = \prod_i \mathrm{PDF}_h^i,\ L_\mu = \prod_i \mathrm{PDF}_\mu^i,$$

where i stands for the index of two types of PDFs and h (μ) for the hadron (muon) likeliness. Here, the two 2D PDFs are known to be correlated (and feasibility of using 3D PDFs is under study). The calculated rlogL distributions are shown for fractional events randomly chosen from the simulated ν_μ CC events in Figure 3. It should be noted that a relative scale between the hadronic and muonic-photon distributions differs event-by-event depending on some factors such as energy split and track length, which may affect the resulting performance. Such impact on individual events will be checked in detail as a future work.

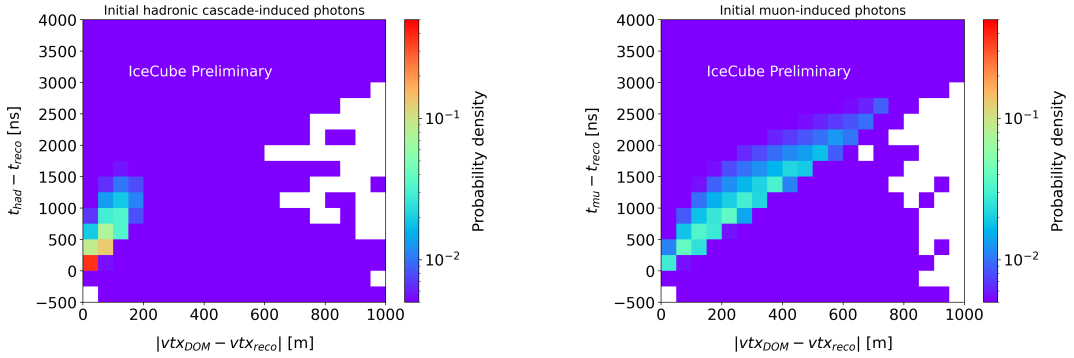

Figure 1: The correlated 2D PDFs of the arrival time of photons as a function of distance from the vertex to DOMs for the hadronic- (left) and muonic-photons (right) produced using the simulated ν_μ CC events.

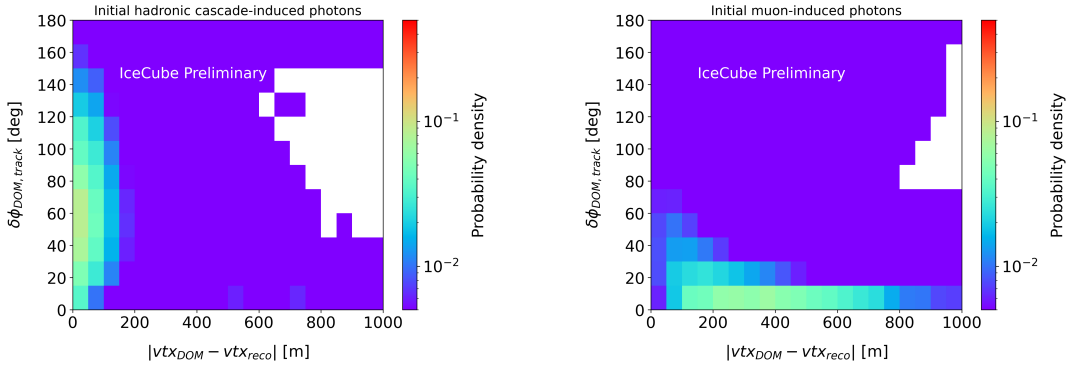

Figure 2: The correlated 2D PDFs of the opening angle between the muon direction and the vertex-to-DOM vector as a function of distance from the vertex to DOMs for the hadronic- (left) and muonic-photons (right) produced using the simulated ν_μ CC events.

PoS(ICRC2023)980

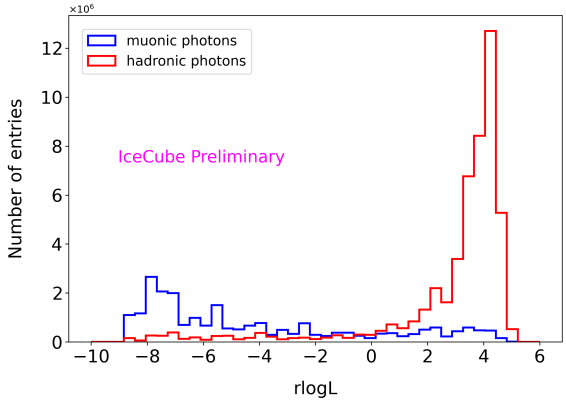

Figure 3: Log-likelihood ratios for the hadronic and muonic photons from the simulated ν_μ CC events. Note that for reconstruction, the direct correspondence beteween photons and pulses is lost and pulses are selected using the photon classification as an approximation. See text for more details.

Table 1: Summary of the pulse samples used in this study.

	Sample (pulse set)	Selection criteria	Application
	Pseudo-cascade	All pulses with 0 < rlogL < 6	Data, MC
MC-truth-based	*Near-cascade*	All hadronic pulses	MC
	Cascade with hadronic pulse loss	Hadronic pulses with 0 < rlogL < 6	MC
	Cascade with muonic pulse contamination	All hadronic pulses and muonic pulses with 0 < rlogL < 6	MC

In IceCube, detected photons are converted into pulses which may contain more photons than one in case those arrive at a DOM in a short time. This processing is performed in MC to make one-to-one comparison to observed data (Data) possible, and information on the parent particle is lost at the pulse level. The rlogL in Figure 3 is based on detected photons and some accuracy is lost when applied to pulses. In this study, multiple sets of pulses are prepared depending on the selection criteria as summarized in Table 1. First, the pulses with 0 < rlogL < 6 are selected and the resulting set is referred to as a *pseudo-cascade* sample. This selection is equally applied to both Data and MC. Another set of pulses which are likely be emitted from the hadronic cascade is prepared based on the MC information. These pulses are selected as ones recorded within ±5 ns from the true hadronic photons (red in Figure 3) and are referred to as a *near-cascade* sample. It may be that this time-based selection also includes pulses generated by the muon or later stochastic losses, as the parent particle association is not preserved at pulse level. This set is used as a truth reference for the *pseudo-cascade* sample. In addition, two more sets of pulses are prepared from MC, so to be able to investigate the impact of the imperfect rlogL-based pulse selection. One of these sets contains only the pulses originating from the hadronic cascade which fall within the 0 < rlogL < 6 selection window. This sample is called *cascade with hadronic pulse loss*. The other set is produced by adding the muon-induced pulses within 0 < rlogL < 6 to the hadronic cascade-induced pulses and referred to as *cascade with muonic pulse contamination*. Note again that these hadronic or muonic

PoS(ICRC2023)980

pulses are selected within a ±5 ns time window around the true hadronic or muonic photon arrivals, respectively. By comparing the results from these two sets with that from the *near-cascade* set, the selection impact can be estimated.

A series of the IceCube cascade reconstruction tools are applied to these pulse sets (see Ref. [8] for the reconstruction updates). For the reconstructions in this study, the ice model Spice BFR-v2 which takes into account the birefringent micro-structure of the ice [9, 10] is used along with the h2-50cm hole ice model. Note that the MC production of the starting track sample is performed based a previous model Spice 3.2.1.

3. Results

The resulting zenith and azimuth directions from the *pseudo-cascade* sample and three MC-truth-based samples are compared with the track directions as shown in Figures 4 and 5, respectively. In zenith, a negative bias is observed in Data and it is larger than that of the MC *pseudo-cascade* sample, while their widths are similar (see the left panel of the figure). In azimuth, no sizable bias is seen in both Data and MC and the widths are comparable.

From comparison between the MC *pseudo-cascade* and MC *near-cascade* samples, it is found that the *pseudo-cascade* bias in zenith is shifted mainly by contamination of the muonic pulses and its resolution in azimuth is deteriorated mainly by loss of the hadronic pulses. The angular resolution, which is derived from the space angle between the reconstructed direction and the true direction, involves both zenith and azimuth. Currently, the angular resolution for *pseudo-cascades* is worse than that for *near-cascades* and this is a subject of further studies; here, only the separate distributions in zenith and azimuth are focused on. With the MC studies performed, it is shown that these distributions can potentially provide hints on the ice modeling.

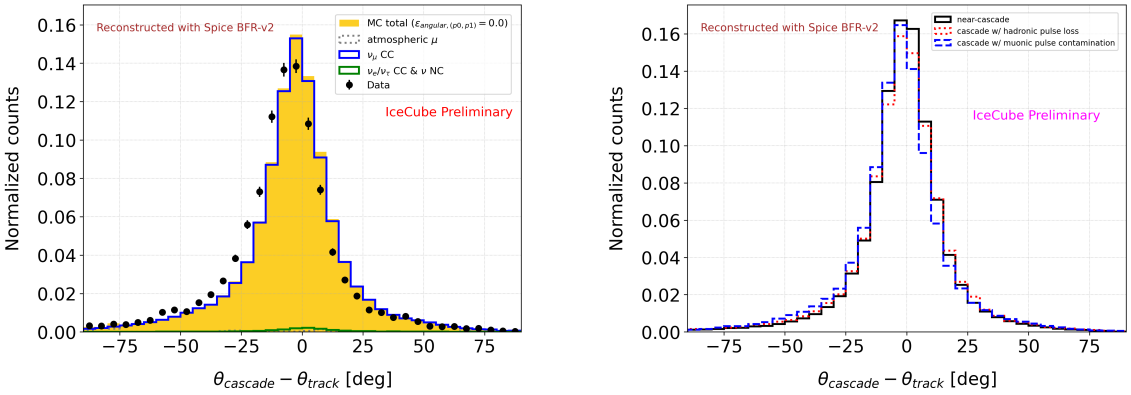

Figure 4: Reconstructed zenith angle difference between cascade and track parts from the *pseudo-cascade* samples for Data and the nominal MC (left) and from the MC-truth-based samples (right). MC distributions are weighted with the best-fit parameters from the ESTES diffuse analysis [4] and all distributions are area normalized. In the left panel, the median and 25%/75% percentiles of the distribution are $-6.3^{+9.8}_{-11.2}$ degrees in Data and $-2.7^{+9.5}_{-10.2}$ degrees in MC. The corresponding ones in the right panel are $-0.9^{+8.4}_{-8.5}$ degrees for black, $-1.0^{+9.1}_{-9.1}$ degrees for red, and $-2.5^{+8.9}_{-9.4}$ degrees for blue distributions.

In the following part, the zenith bias is discussed in more details. Since the bias obtained from the Data distribution in the left panel of Figure 4 is for *pseudo-cascades*, it is corrected for the

PoS(ICRC2023)980

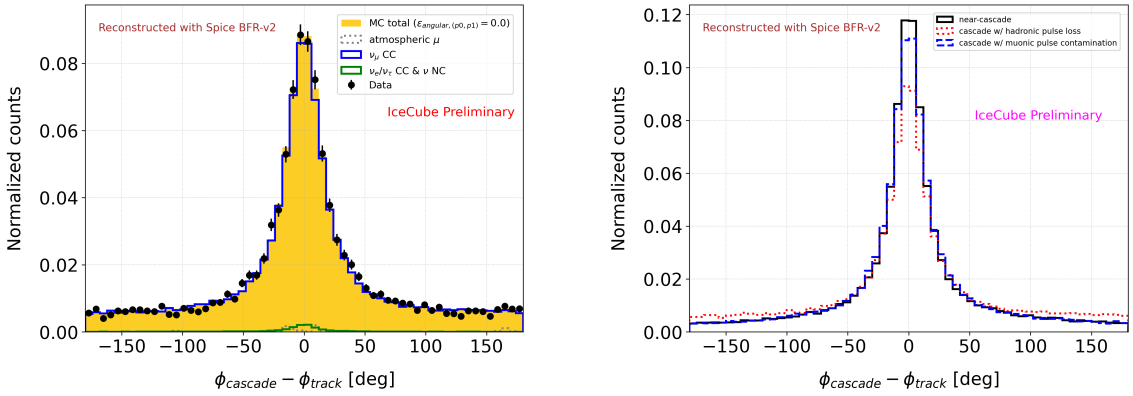

Figure 5: Same as Figure 4 but for azimuth. In the left panel, the median and 25%/75% percentiles of the distribution are $0.4^{+24.3}_{-23.5}$ degrees in Data and $0.0^{+23.9}_{-23.3}$ degrees in MC. The corresponding ones in the right panel are $0.1^{+17.3}_{-16.9}$ degrees for black, $0.1^{+24.8}_{-23.6}$ degrees for red, and $0.1^{+18.2}_{-17.8}$ degrees for blue distributions.

impacts from the rlogL-based pulse selection to be compared to the *near-cascade* result in a fair way. This is performed by the formula: $\Delta_{\text{corrected}} = \Delta_{\text{pseudocasc}} - (\Delta_{\text{hadloss}} - \Delta_{\text{casc}}) - (\Delta_{\text{mucontami}} - \Delta_{\text{casc}})$. Here, $\Delta_{\text{pseudocasc}}$ is the median of the *pseudo-cascade* distributions (left panel of Figure 4) and considered for Data and MC as $\Delta_{\text{pseudocasc,Data}}$ and $\Delta_{\text{pseudocasc,MC}}$, respectively. The correction part is composed of three medians, Δ_{casc}, Δ_{hadloss}, and $\Delta_{\text{mucontami}}$, from the *near-cascade*, *cascade with hadronic pulse loss*, and *cascade with muonic pulse contamination* distributions in the right panel of Figure 4. $\Delta_{\text{corrected,MC}}$ is compared with the *near-cascade* result (Δ_{casc}) on purpose of validating the correction formula above because its form is essentially a guess. The median of each distribution is obtained for ν_μ CC events and this is achieved for Data with a subtraction of the non-ν_μ CC contribution using MC with considering the relative total number of events between Data and MC. It should be mentioned that the correction effect by this formula is not large in the present study, but still it is applied for the later results.

In the correction formula, Δ_{casc}, Δ_{hadloss}, and $\Delta_{\text{mucontami}}$ are affected by systematic uncertainties regarding physics and detector modeling. A major source of systematic uncertainty is the parametrization of the so-called hole ice, the refrozen column of ice in which DOMs are installed, where the photon propagation differs from that in the bulk ice (see Ref. [11] for more details about the hole ice). Figure 6 shows the zenith bias resulting from MC simulation sets with different assumed hole ice parameters, $\epsilon_{\text{angular},p0}$ and $\epsilon_{\text{angular},p1}$. It is found that the zenith bias is largely sensitive to both of the hole ice parameters. The h2-50cm model is used in the reconstruction and corresponds roughly to $(\epsilon_{\text{angular},p0}, \epsilon_{\text{angular},p1}) = (-0.4, 0.075)$ in the new parametrization scheme. The impacts of all considered systematic uncertainties are shown in Figure 7. The effect of uncertainties relating to the physics modeling is small in comparison to detector systematic uncertainties. The largest impact comes from hole ice parameters; however, their effect on the converted results from Data is not sizable enough to fully compensate the observed bias from zero. Consistent values of the converted results from the MC *pseudo-cascade* and the MC *near-cascade* results ensure that the assumption about the correction formula in this study is reasonable.

The results for different zenith regions, $-1.0 < \cos\theta_{\text{zenith}} < -0.5$, $-0.5 < \cos\theta_{\text{zenith}} < 0.0$, and $0.0 < \cos\theta_{\text{zenith}} < 0.5$, are shown in Figure 8. As a reference, the MC *near-cascade* results with

PoS(ICRC2023)980

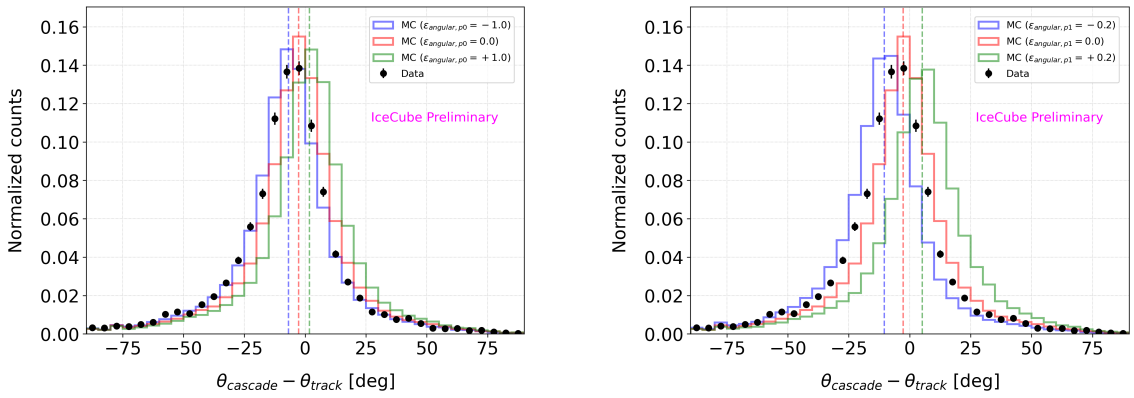

Figure 6: Zenith bias from the MC production with different choices of hole ice parameters, $\epsilon_{\text{angular},p0}$ (left) and $\epsilon_{\text{angular},p1}$ (right), in comparison with that from Data. In the left and right panels, $\epsilon_{\text{angular},p1}$ and $\epsilon_{\text{angular},p0}$ are set to 0.0, respectively. Dashed lines represent the median of each MC distribution.

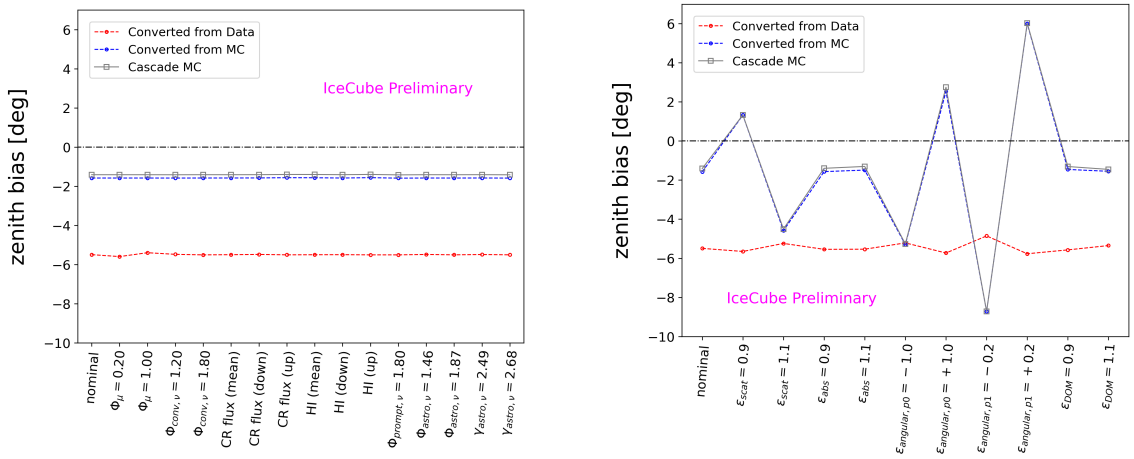

Figure 7: Zenith bias with the correction formula based on the nominal MC and the different systematic uncertainties. The left and right panels correspond to the cases with physics and detector systematic uncertainties, respectively. In each panel, the converted results from the Data *pseudo-cascade* (red), the converted results from the MC *pseudo-cascade* (blue), and the MC *near-cascade* results (grey) are shown.

different hole ice parameters are also plotted (the converted results from the MC *pseudo-cascade* are consistent with the MC *near-cascade* results as seen in Figure 7). Note that the ν_μ CC purity differs bin-by-bin and so does the subtraction effect. The observed zenith bias based on Data is significantly negative in every bin and its size is larger for northern sky events. The zenith bias dependence on deposited energy of the hadronic part of ν_μ CC events is also investigated and no strong dependence is found for the region of 10^2–10^4 GeV. These dependence could be a key to understanding the ice features and further improvement of the IceCube reconstruction tool.

4. Conclusion and Outlook

In this study, a data-based method is employed on the ESTES neutrino source search sample to compare per-event reconstructions of cascade-like pulses against that of the full event. Two types

PoS(ICRC2023)980

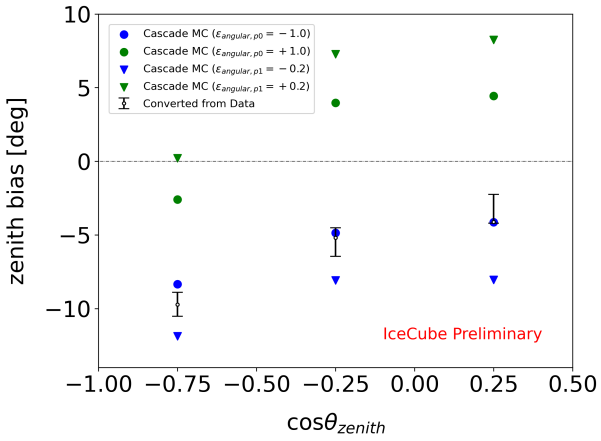

Figure 8: Zenith bias converted from the Data *pseudo-cascade* with systematic uncertainties for different cosine zenith bins in comparison with the MC *near-cascade* results with different hole ice parameters. Note that $\epsilon_{\text{angular},p1}$ is set to 0.0 for the case of $\epsilon_{\text{angular},p0} = \pm 1.0$ and $\epsilon_{\text{angular},p0}$ is set to 0.0 for $\epsilon_{\text{angular},p1} = \pm 0.2$.

of 2D PDFs are employed to calculate log-likelihood ratios for selecting Cherenkov photons from the initial hadronic cascade in ν_μ CC events. Noting that the correspondence between photons and pulses is not one-to-one, different sets of pulses are selected based on these log-likelihood ratios and passed to angular reconstruction. The resulting zenith and azimuth directions are then compared to the reconstructed track zenith and azimuth. In particular, the zenith bias derived from the *pseudo-cascade* sample is converted to the bias for cascades using MC-truth-based samples. Here, systematic uncertainties regarding physics and detector modeling are considered. The results imply that a modification of the hole ice can describe observed data better, but the effect is not completely understood and further studies are needed.

References

[1] **IceCube** Collaboration, M. G. Aartsen *et al.* *PRL* **113** no. 10, (2014) 101101.

[2] **IceCube** Collaboration, M. G. Aartsen *et al.* *PRD* **89** no. 10, (2014) 102004.

[3] **IceCube** Collaboration, M. G. Aartsen *et al.* *PRD* **99** no. 3, (2019) 032004.

[4] **IceCube** Collaboration, M. Silva and S. Mancina *PoS* **ICRC2019** (2019) 1010.

[5] **IceCube** Collaboration, S. Mancina and M. Silva *PoS* **ICRC2019** (2019) 954.

[6] **IceCube** Collaboration, M. Silva and S. Mancina *PoS* **ICRC2021** (2021) 1130.

[7] **IceCube** Collaboration, M. Silva *et al. PoS* **ICRC2023** (these proceedings) 1008.

[8] **IceCube** Collaboration, T. Yuan *NIM A* **1054** (2023) 168440.

[9] **IceCube** Collaboration, M. Rongen and D. Chirkin *PoS* **ICRC2021** (2021) 1119.

[10] **IceCube** Collaboration, R. Abbasi *et al.* *Submitted to The CryoSphere* .

[11] **IceCube** Collaboration, P. Eller and M. Rongen *PoS* **ICRC2023** (these proceedings) 1034.

PoS(ICRC2023)980

Full Author List: IceCube Collaboration

R. Abbasi[17], M. Ackermann[63], J. Adams[18], S. K. Agarwalla[40, 64], J. A. Aguilar[12], M. Ahlers[22], J.M. Alameddine[23], N. M. Amin[44], K. Andeen[42], G. Anton[26], C. Argüelles[14], Y. Ashida[53], S. Athanasiadou[63], S. N. Axani[44], X. Bai[50], A. Balagopal V.[40], M. Baricevic[40], S. W. Barwick[30], V. Basu[40], R. Bay[8], J. J. Beatty[20, 21], J. Becker Tjus[11, 65], J. Beise[61], C. Bellenghi[27], C. Benning[1], S. BenZvi[52], D. Berley[19], E. Bernardini[48], D. Z. Besson[36], E. Blaufuss[19], S. Blot[63], F. Bontempo[31], J. Y. Book[14], C. Boscolo Meneguolo[48], S. Böser[41], O. Botner[61], J. Böttcher[1], E. Bourbeau[22], J. Braun[40], B. Brinson[6], J. Brostean-Kaiser[63], R. T. Burley[2], R. S. Busse[43], D. Butterfield[40], M. A. Campana[49], K. Carloni[14], E. G. Carnie-Bronca[2], S. Chattopadhyay[40, 64], N. Chau[12], C. Chen[6], Z. Chen[55], D. Chirkin[40], S. Choi[56], B. A. Clark[19], L. Classen[43], A. Coleman[61], G. H. Collin[15], A. Connolly[20, 21], J. M. Conrad[15], P. Coppin[13], P. Correa[13], D. F. Cowen[59, 60], P. Dave[6], C. De Clercq[13], J. J. DeLaunay[58], D. Delgado[14], S. Deng[1], K. Deoskar[54], A. Desai[40], P. Desiati[40], K. D. de Vries[13], G. de Wasseige[37], T. DeYoung[24], A. Diaz[15], J. C. Díaz-Vélez[40], M. Dittmer[43], A. Domi[26], H. Dujmovic[40], M. A. DuVernois[40], T. Ehrhardt[41], P. Eller[27], E. Ellinger[62], S. El Mentawi[1], D. Elsässer[23], R. Engel[31, 32], H. Erpenbeck[40], J. Evans[19], P. A. Evenson[44], K. L. Fan[19], K. Fang[40], K. Farrag[16], A. R. Fazely[7], A. Fedynitch[57], N. Feigl[10], S. Fiedlschuster[26], C. Finley[54], L. Fischer[63], D. Fox[59], A. Franckowiak[11], A. Fritz[41], P. Fürst[1], J. Gallagher[39], E. Ganster[1], A. Garcia[14], L. Gerhardt[9], A. Ghadimi[58], C. Glaser[61], T. Glauch[27], T. Glüsenkamp[26, 61], N. Goehlke[32], J. G. Gonzalez[44], S. Goswami[58], D. Grant[24], S. J. Gray[19], O. Gries[1], S. Griffin[40], S. Griswold[52], K. M. Groth[22], C. Günther[1], P. Gutjahr[23], C. Haack[26], A. Hallgren[61], R. Halliday[24], L. Halve[1], F. Halzen[40], H. Hamdaoui[55], M. Ha Minh[27], K. Hanson[40], J. Hardin[15], A. A. Harnisch[24], P. Hatch[33], A. Haungs[31], K. Helbing[62], J. Hellrung[11], F. Henningsen[27], L. Heuermann[1], N. Heyer[61], S. Hickford[62], A. Hidvegi[54], C. Hill[16], G. C. Hill[2], K. D. Hoffman[19], S. Hori[40], K. Hoshina[40, 66], W. Hou[31], T. Huber[31], K. Hultqvist[54], M. Hünnefeld[23], R. Hussain[40], K. Hymon[23], S. In[56], A. Ishihara[16], M. Jacquart[40], O. Janik[1], M. Jansson[54], G. S. Japaridze[5], M. Jeong[56], M. Jin[14], B. J. P. Jones[4], D. Kang[31], W. Kang[56], X. Kang[49], A. Kappes[43], D. Kappesser[41], L. Kardum[23], T. Karg[63], M. Karl[27], A. Karle[40], U. Katz[26], M. Kauer[40], J. L. Kelley[40], A. Khatee Zathul[40], A. Kheirandish[34, 35], J. Kiryluk[55], S. R. Klein[8, 9], A. Kochocki[24], R. Koirala[44], H. Kolanoski[10], T. Kontrimas[27], L. Köpke[41], C. Kopper[26], D. J. Koskinen[22], P. Koundal[31], M. Kovacevich[49], M. Kowalski[10, 63], T. Kozynets[22], J. Krishnamoorthi[40, 64], K. Kruiswijk[37], E. Krupczak[24], A. Kumar[63], E. Kun[11], N. Kurahashi[49], N. Lad[63], C. Lagunas Gualda[63], M. Lamoureux[37], M. J. Larson[19], S. Latseva[1], F. Lauber[62], J. P. Lazar[14, 40], J. W. Lee[56], K. Leonard DeHolton[60], A. Leszczyńska[44], M. Lincetto[11], Q. R. Liu[40], M. Liubarska[25], E. Lohfink[41], C. Love[49], C. J. Lozano Mariscal[43], L. Lu[40], F. Lucarelli[28], W. Luszczak[20, 21], Y. Lyu[8, 9], J. Madsen[40], K. B. M. Mahn[24], Y. Makino[40], E. Manao[27], S. Mancina[40, 48], W. Marie Sainte[40], I. C. Mariş[12], S. Marka[46], Z. Marka[46], M. Marsee[58], I. Martinez-Soler[14], R. Maruyama[45], F. Mayhew[24], T. McElroy[25], F. McNally[38], J. V. Mead[22], K. Meagher[40], S. Mechbal[63], A. Medina[21], M. Meier[16], Y. Merckx[13], L. Merten[11], J. Micallef[24], J. Mitchell[7], T. Montaruli[28], R. W. Moore[25], Y. Morii[16], R. Morse[40], M. Moulai[40], T. Mukherjee[31], R. Naab[63], R. Nagai[16], M. Nakos[40], U. Naumann[62], J. Necker[63], A. Negi[4], M. Neumann[43], H. Niederhausen[24], M. U. Nisa[24], A. Noell[1], A. Novikov[44], S. C. Nowicki[24], A. Obertacke Pollmann[16], V. O'Dell[40], M. Oehler[31], B. Oeyen[29], A. Olivas[19], R. Ørsøe[27], J. Osborn[40], E. O'Sullivan[61], H. Pandya[44], N. Park[33], G. K. Parker[4], E. N. Paudel[44], L. Paul[42, 50], C. Pérez de los Heros[61], J. Peterson[40], S. Philippen[1], A. Pizzuto[40], M. Plum[50], A. Pontén[61], Y. Popovych[41], M. Prado Rodriguez[40], B. Pries[24], R. Procter-Murphy[19], G. T. Przybylski[9], C. Raab[37], J. Rack-Helleis[41], K. Rawlins[3], Z. Rechav[40], A. Rehman[44], P. Reichherzer[11], G. Renzi[12], E. Resconi[27], S. Reusch[63], W. Rhode[23], B. Riedel[40], A. Rifaie[1], E. J. Roberts[2], S. Robertson[8, 9], S. Rodan[56], G. Roellinghoff[56], M. Rongen[26], C. Rott[53, 56], T. Ruhe[23], L. Ruohan[27], D. Ryckbosch[29], I. Safa[14, 40], J. Saffer[32], D. Salazar-Gallegos[24], P. Sampathkumar[31], S. E. Sanchez Herrera[24], A. Sandrock[62], M. Santander[58], S. Sarkar[25], S. Sarkar[47], J. Savelberg[1], P. Savina[40], M. Schaufel[1], H. Schieler[31], S. Schindler[26], L. Schlickmann[1], B. Schlüter[43], F. Schlüter[12], N. Schmeisser[62], T. Schmidt[19], J. Schneider[26], F. G. Schröder[31, 44], L. Schumacher[26], G. Schwefer[1], S. Sclafani[19], D. Seckel[44], M. Seikh[36], S. Seunarine[51], R. Shah[49], A. Sharma[61], S. Shefali[32], N. Shimizu[16], M. Silva[40], B. Skrzypek[14], B. Smithers[4], R. Snihur[40], J. Soedingrekso[23], A. Søgaard[22], D. Soldin[32], P. Soldin[1], G. Sommani[11], C. Spannfellner[27], G. M. Spiczak[51], C. Spiering[63], M. Stamatikos[21], T. Stanev[44], T. Stezelberger[9], T. Stürwald[62], T. Stuttard[22], G. W. Sullivan[19], I. Taboada[6], S. Ter-Antonyan[7], M. Thiesmeyer[1], W. G. Thompson[14], J. Thwaites[40], S. Tilav[44], K. Tollefson[24], C. Tönnis[56], S. Toscano[12], D. Tosi[40], A. Trettin[63], C. F. Tung[6], R. Turcotte[31], J. P. Twagirayezu[24], B. Ty[40], M. A. Unland Elorrieta[43], A. K. Upadhyay[40, 64], K. Upshaw[7], N. Valtonen-Mattila[61], J. Vandenbroucke[40], N. van Eijndhoven[13], D. Vannerom[15], J. van Santen[63], J. Vara[43], J. Veitch-Michaelis[40], M. Venugopal[31], M. Vereecken[37], S. Verpoest[44], D. Veske[46], A. Vijai[19], C. Walck[54], C. Weaver[24], P. Weigel[15], A. Weindl[31], J. Weldert[60], C. Wendt[40], J. Werthebach[23], M. Weyrauch[31], N. Whitehorn[24], C. H. Wiebusch[1], N. Willey[24], D. R. Williams[58], L. Witthaus[23], A. Wolf[1], M. Wolf[27], G. Wrede[26], X. W. Xu[7], J. P. Yanez[25], E. Yildizci[40], S. Yoshida[16], R. Young[36], F. Yu[14], S. Yu[24], T. Yuan[40], Z. Zhang[55], P. Zhelnin[14], M. Zimmerman[40]

[1] III. Physikalisches Institut, RWTH Aachen University, D-52056 Aachen, Germany
[2] Department of Physics, University of Adelaide, Adelaide, 5005, Australia
[3] Dept. of Physics and Astronomy, University of Alaska Anchorage, 3211 Providence Dr., Anchorage, AK 99508, USA
[4] Dept. of Physics, University of Texas at Arlington, 502 Yates St., Science Hall Rm 108, Box 19059, Arlington, TX 76019, USA
[5] CTSPS, Clark-Atlanta University, Atlanta, GA 30314, USA
[6] School of Physics and Center for Relativistic Astrophysics, Georgia Institute of Technology, Atlanta, GA 30332, USA
[7] Dept. of Physics, Southern University, Baton Rouge, LA 70813, USA
[8] Dept. of Physics, University of California, Berkeley, CA 94720, USA
[9] Lawrence Berkeley National Laboratory, Berkeley, CA 94720, USA
[10] Institut für Physik, Humboldt-Universität zu Berlin, D-12489 Berlin, Germany
[11] Fakultät für Physik & Astronomie, Ruhr-Universität Bochum, D-44780 Bochum, Germany
[12] Université Libre de Bruxelles, Science Faculty CP230, B-1050 Brussels, Belgium

PoS(ICRC2023)980

[13] Vrije Universiteit Brussel (VUB), Dienst ELEM, B-1050 Brussels, Belgium
[14] Department of Physics and Laboratory for Particle Physics and Cosmology, Harvard University, Cambridge, MA 02138, USA
[15] Dept. of Physics, Massachusetts Institute of Technology, Cambridge, MA 02139, USA
[16] Dept. of Physics and The International Center for Hadron Astrophysics, Chiba University, Chiba 263-8522, Japan
[17] Department of Physics, Loyola University Chicago, Chicago, IL 60660, USA
[18] Dept. of Physics and Astronomy, University of Canterbury, Private Bag 4800, Christchurch, New Zealand
[19] Dept. of Physics, University of Maryland, College Park, MD 20742, USA
[20] Dept. of Astronomy, Ohio State University, Columbus, OH 43210, USA
[21] Dept. of Physics and Center for Cosmology and Astro-Particle Physics, Ohio State University, Columbus, OH 43210, USA
[22] Niels Bohr Institute, University of Copenhagen, DK-2100 Copenhagen, Denmark
[23] Dept. of Physics, TU Dortmund University, D-44221 Dortmund, Germany
[24] Dept. of Physics and Astronomy, Michigan State University, East Lansing, MI 48824, USA
[25] Dept. of Physics, University of Alberta, Edmonton, Alberta, Canada T6G 2E1
[26] Erlangen Centre for Astroparticle Physics, Friedrich-Alexander-Universität Erlangen-Nürnberg, D-91058 Erlangen, Germany
[27] Technical University of Munich, TUM School of Natural Sciences, Department of Physics, D-85748 Garching bei München, Germany
[28] Département de physique nucléaire et corpusculaire, Université de Genève, CH-1211 Genève, Switzerland
[29] Dept. of Physics and Astronomy, University of Gent, B-9000 Gent, Belgium
[30] Dept. of Physics and Astronomy, University of California, Irvine, CA 92697, USA
[31] Karlsruhe Institute of Technology, Institute for Astroparticle Physics, D-76021 Karlsruhe, Germany
[32] Karlsruhe Institute of Technology, Institute of Experimental Particle Physics, D-76021 Karlsruhe, Germany
[33] Dept. of Physics, Engineering Physics, and Astronomy, Queen's University, Kingston, ON K7L 3N6, Canada
[34] Department of Physics & Astronomy, University of Nevada, Las Vegas, NV, 89154, USA
[35] Nevada Center for Astrophysics, University of Nevada, Las Vegas, NV 89154, USA
[36] Dept. of Physics and Astronomy, University of Kansas, Lawrence, KS 66045, USA
[37] Centre for Cosmology, Particle Physics and Phenomenology - CP3, Université catholique de Louvain, Louvain-la-Neuve, Belgium
[38] Department of Physics, Mercer University, Macon, GA 31207-0001, USA
[39] Dept. of Astronomy, University of Wisconsin–Madison, Madison, WI 53706, USA
[40] Dept. of Physics and Wisconsin IceCube Particle Astrophysics Center, University of Wisconsin–Madison, Madison, WI 53706, USA
[41] Institute of Physics, University of Mainz, Staudinger Weg 7, D-55099 Mainz, Germany
[42] Department of Physics, Marquette University, Milwaukee, WI, 53201, USA
[43] Institut für Kernphysik, Westfälische Wilhelms-Universität Münster, D-48149 Münster, Germany
[44] Bartol Research Institute and Dept. of Physics and Astronomy, University of Delaware, Newark, DE 19716, USA
[45] Dept. of Physics, Yale University, New Haven, CT 06520, USA
[46] Columbia Astrophysics and Nevis Laboratories, Columbia University, New York, NY 10027, USA
[47] Dept. of Physics, University of Oxford, Parks Road, Oxford OX1 3PU, United Kingdom
[48] Dipartimento di Fisica e Astronomia Galileo Galilei, Università Degli Studi di Padova, 35122 Padova PD, Italy
[49] Dept. of Physics, Drexel University, 3141 Chestnut Street, Philadelphia, PA 19104, USA
[50] Physics Department, South Dakota School of Mines and Technology, Rapid City, SD 57701, USA
[51] Dept. of Physics, University of Wisconsin, River Falls, WI 54022, USA
[52] Dept. of Physics and Astronomy, University of Rochester, Rochester, NY 14627, USA
[53] Department of Physics and Astronomy, University of Utah, Salt Lake City, UT 84112, USA
[54] Oskar Klein Centre and Dept. of Physics, Stockholm University, SE-10691 Stockholm, Sweden
[55] Dept. of Physics and Astronomy, Stony Brook University, Stony Brook, NY 11794-3800, USA
[56] Dept. of Physics, Sungkyunkwan University, Suwon 16419, Korea
[57] Institute of Physics, Academia Sinica, Taipei, 11529, Taiwan
[58] Dept. of Physics and Astronomy, University of Alabama, Tuscaloosa, AL 35487, USA
[59] Dept. of Astronomy and Astrophysics, Pennsylvania State University, University Park, PA 16802, USA
[60] Dept. of Physics, Pennsylvania State University, University Park, PA 16802, USA
[61] Dept. of Physics and Astronomy, Uppsala University, Box 516, S-75120 Uppsala, Sweden
[62] Dept. of Physics, University of Wuppertal, D-42119 Wuppertal, Germany
[63] Deutsches Elektronen-Synchrotron DESY, Platanenallee 6, 15738 Zeuthen, Germany
[64] Institute of Physics, Sachivalaya Marg, Sainik School Post, Bhubaneswar 751005, India
[65] Department of Space, Earth and Environment, Chalmers University of Technology, 412 96 Gothenburg, Sweden
[66] Earthquake Research Institute, University of Tokyo, Bunkyo, Tokyo 113-0032, Japan

Acknowledgements

The authors gratefully acknowledge the support from the following agencies and institutions: USA – U.S. National Science Foundation-Office of Polar Programs, U.S. National Science Foundation-Physics Division, U.S. National Science Foundation-EPSCoR, Wisconsin Alumni Research Foundation, Center for High Throughput Computing (CHTC) at the University of Wisconsin–Madison, Open Science

PoS(ICRC2023)980

Grid (OSG), Advanced Cyberinfrastructure Coordination Ecosystem: Services & Support (ACCESS), Frontera computing project at the Texas Advanced Computing Center, U.S. Department of Energy-National Energy Research Scientific Computing Center, Particle astrophysics research computing center at the University of Maryland, Institute for Cyber-Enabled Research at Michigan State University, and Astroparticle physics computational facility at Marquette University; Belgium – Funds for Scientific Research (FRS-FNRS and FWO), FWO Odysseus and Big Science programmes, and Belgian Federal Science Policy Office (Belspo); Germany – Bundesministerium für Bildung und Forschung (BMBF), Deutsche Forschungsgemeinschaft (DFG), Helmholtz Alliance for Astroparticle Physics (HAP), Initiative and Networking Fund of the Helmholtz Association, Deutsches Elektronen Synchrotron (DESY), and High Performance Computing cluster of the RWTH Aachen; Sweden – Swedish Research Council, Swedish Polar Research Secretariat, Swedish National Infrastructure for Computing (SNIC), and Knut and Alice Wallenberg Foundation; European Union – EGI Advanced Computing for research; Australia – Australian Research Council; Canada – Natural Sciences and Engineering Research Council of Canada, Calcul Québec, Compute Ontario, Canada Foundation for Innovation, WestGrid, and Compute Canada; Denmark – Villum Fonden, Carlsberg Foundation, and European Commission; New Zealand – Marsden Fund; Japan – Japan Society for Promotion of Science (JSPS) and Institute for Global Prominent Research (IGPR) of Chiba University; Korea – National Research Foundation of Korea (NRF); Switzerland – Swiss National Science Foundation (SNSF); United Kingdom – Department of Physics, University of Oxford.

PoS(ICRC2023)980